Supporting Information

Self-assembly Ultrathin Film of CNC/PVA-Liquid Metal Composite as Multifunctional Janus Material

*Pengju Zhang, † Qian Wang, † Rui Guo, Mingkuan Zhang, Shunqi Wang, Chennan Lu, Mianqi Xue, Junbing Fan, Zhizhu He, * Wei Rao**

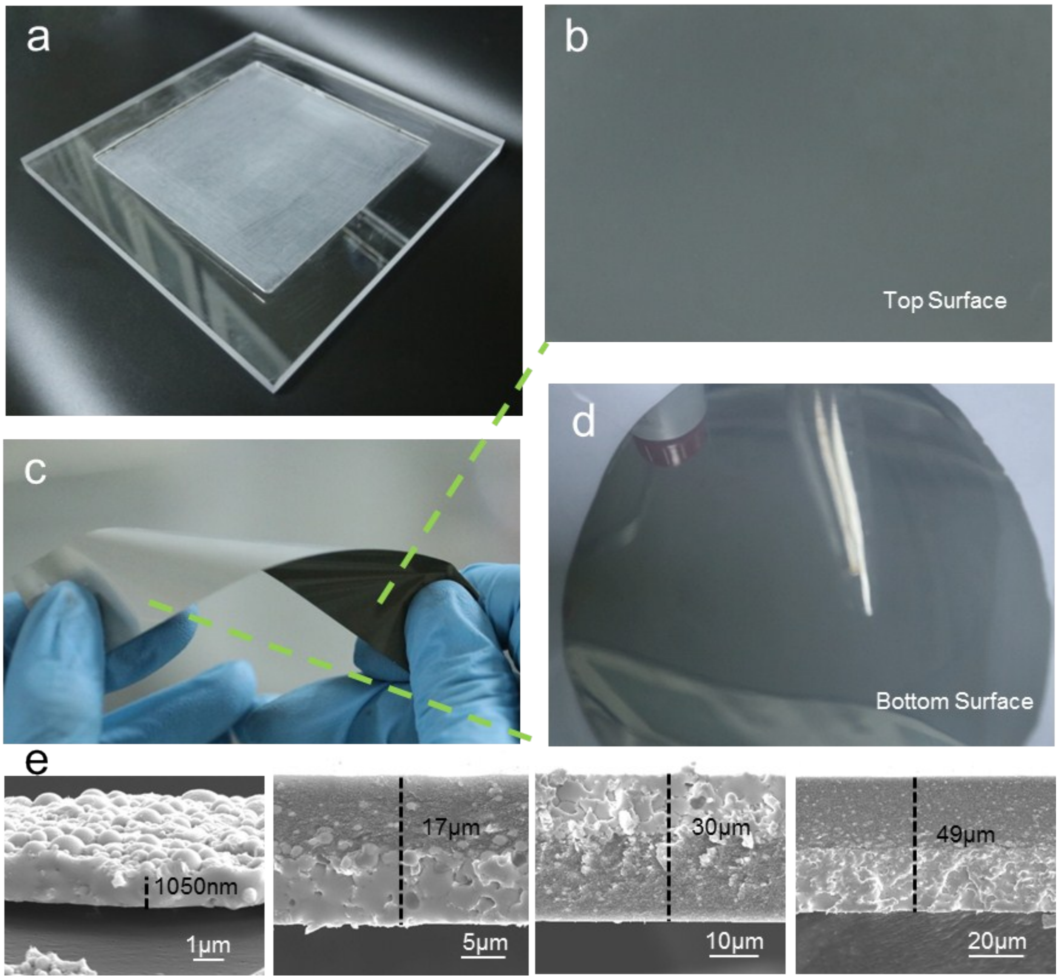

Figure S1. Details of PCLM fabrication process and macro view of Janus film. a) LM Janus film forming template. b) The LM Janus film. c) Macro view of the top surface. d) Macro view of the bottom surface. e) Cross-section of Janus film with different thickness.

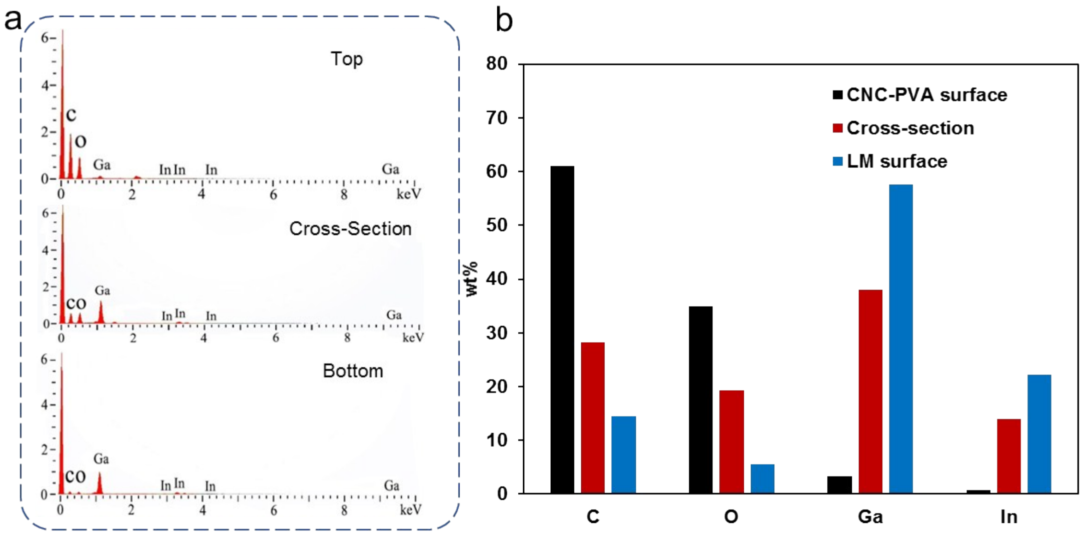

Figure S2. Energy spectrum of the top surface, cross-section and the bottom surface of the film. a) Energy spectrum of the top surface, cross-section and the bottom surface of the film. b) The content difference of C, O, Ga and In elements on the top surface (CNC-PVA surface), cross-section and the bottom surface (LM surface) of the film.

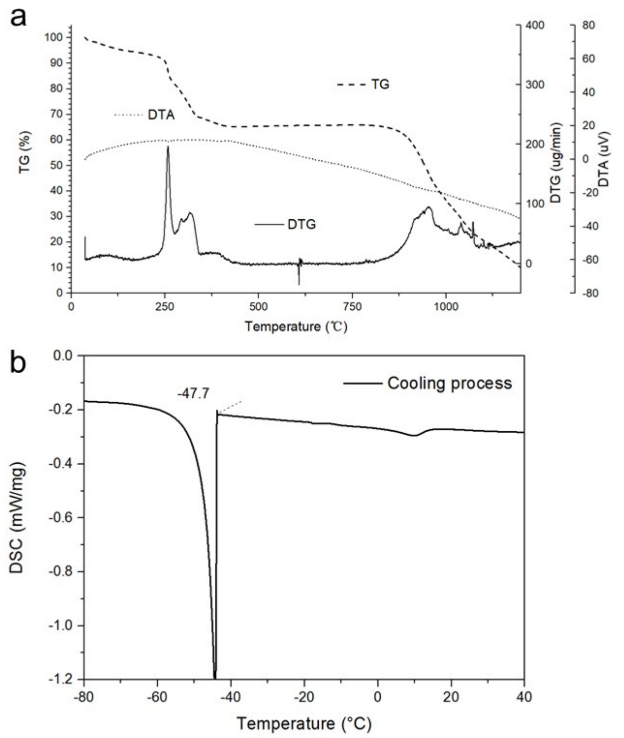

Figure S3. Thermogravimetry and cooling test. a) Thermogravimetric analysis. b) Phase transition point test.

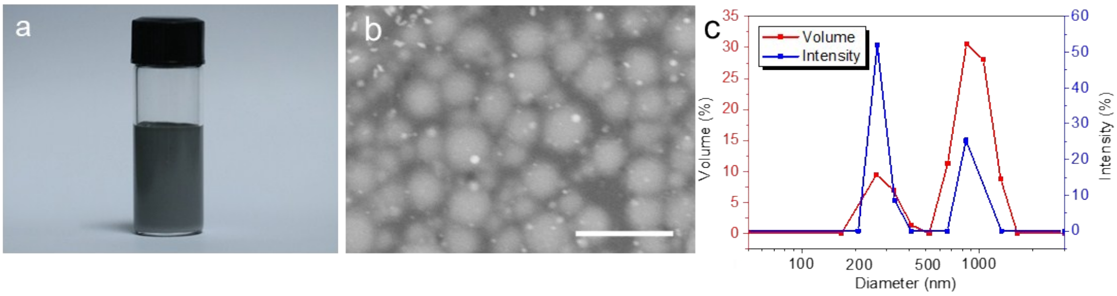

Figure S4. Characteristics of PVC/CNC-LM mixture solution. a) Prepared suspension solution composed of LM micro/nano particles, PVA and CNC. b) Microscopic morphology of the suspension solution. Scale bar: 3μm. c) Particle size distribution in the LM slurry considering both intensity and volume of particles. DLS test results display the average particle size is 489.7±41.8 nm, while the average particle size by intensity is 554.4±102.6 nm, the average particle size by volume is 782.0±142.3 nm.

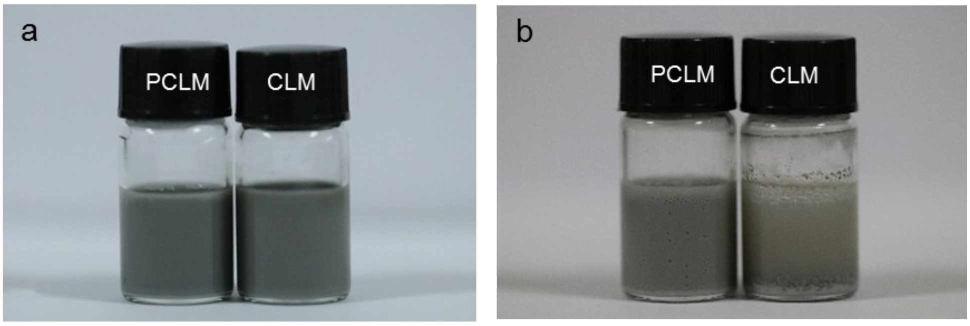

Figure S5. Comparation of stability between the PCLM and CLM solutions. a) 0-day standing after the suspension produced by ultrasonic the mixture of different components. b) Two-weeks standing after the suspension obtained.

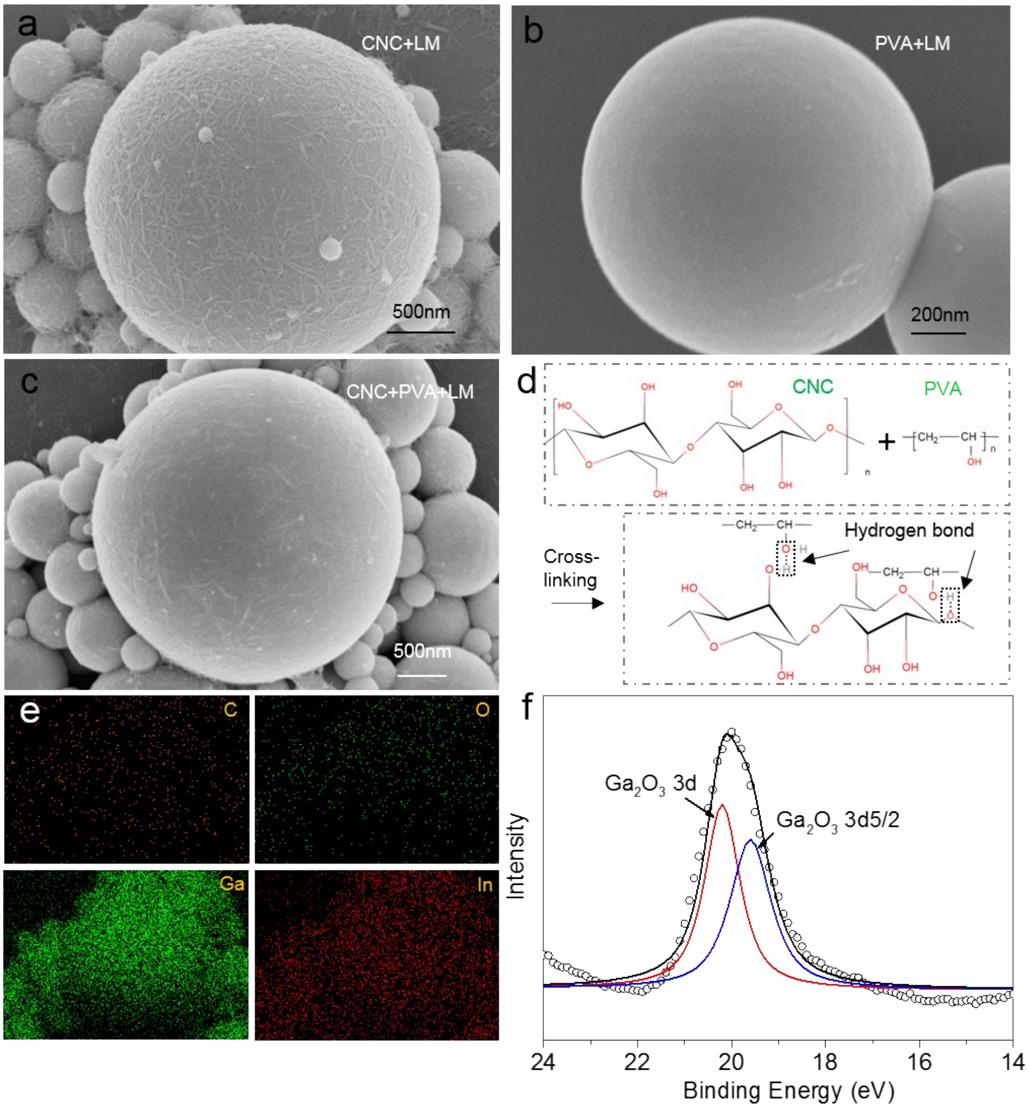

Figure S6. SEM image of the surface of liquid metal microspheres obtained by sonicating the mixture of CNC and liquid metal. b. SEM image of the surface of liquid metal microspheres obtained by sonicating the mixture of PVA and liquid metal. c. SEM image of the surface of liquid metal microspheres obtained by sonicating the mixture of CNC and PVA and liquid metal. The chart inset is the result of EDS mapping of elemental mass content of the liquid metal microspheres. d. Cross-linking reaction of CNC and PVA. e. The EDS spectrum of the surface of the liquid metal microspheres showing the distribution of C, O, Ga, and In on the surface of liquid metal microspheres. f. XPS analysis of Ga 3d of the surface of liquid metal microspheres.

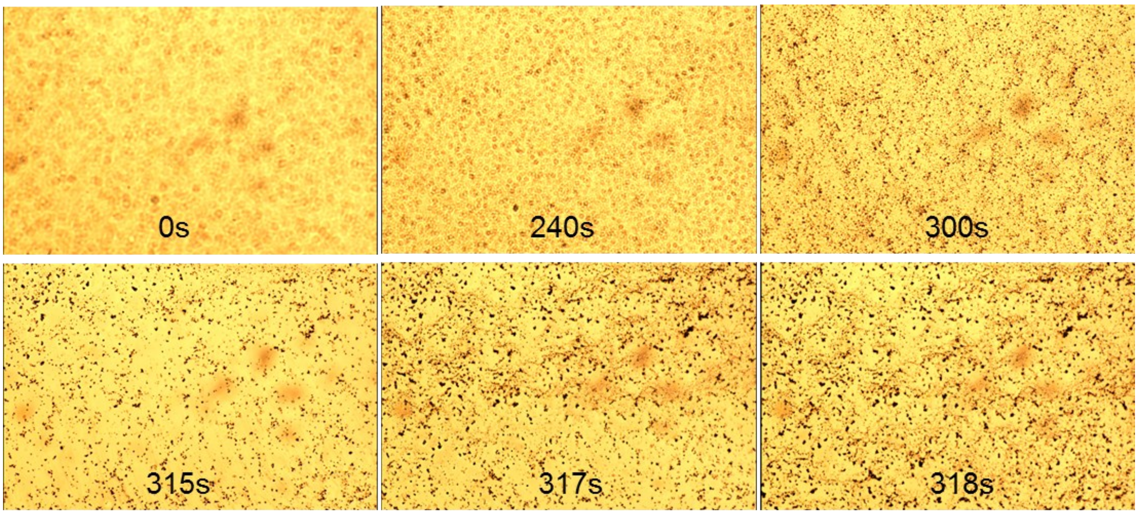

Figure S7. Microscopic images of the natural deposition process of LM particles. At the beginning, the LM particles suspended in the droplet look blurry in the field of view (image at t=0 s). As the water in the droplets evaporated, LM particles started to gather together and the number of particles in the microscopic field increased significantly (image at t=248 s). Soon afterwards, the process of particle deposition was accelerated, then, the particles were clearer in the field of view (image at t=259 s). At 291 s, the water in the droplet was about to evaporate completely. Images similar to a big storm can be seen from 291 s to 309 s owing to the movement of particles in the droplets driven by the surface tension of the water droplets and the air interface which can be seen in Movie S2. At 309 s, the particles in the droplet were all deposited at the bottom. The interaction forces among PVA, CNC and water enable LM micro/nano particles to be stably dispersed in solution. However, as the evaporation process progresses, the interaction forces gradually decrease and is insufficient to support the gravity of LM micro/nano particles. As a result, the LM micro/nano particles start to sink and eventually settle to the bottom. The CNC and PVA are relatively light, so that they mainly distribute in the upper layer.

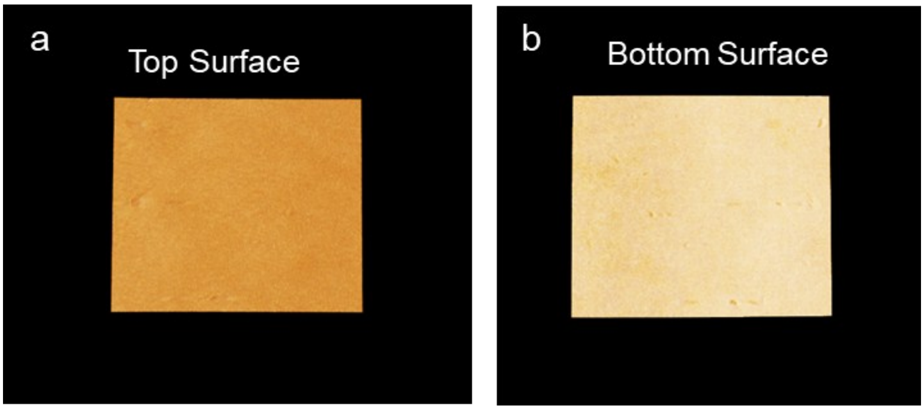

Figure S8. CT images showing the density distribution of LM Janus film. a) View of the top surface. b) View of the bottom surface.

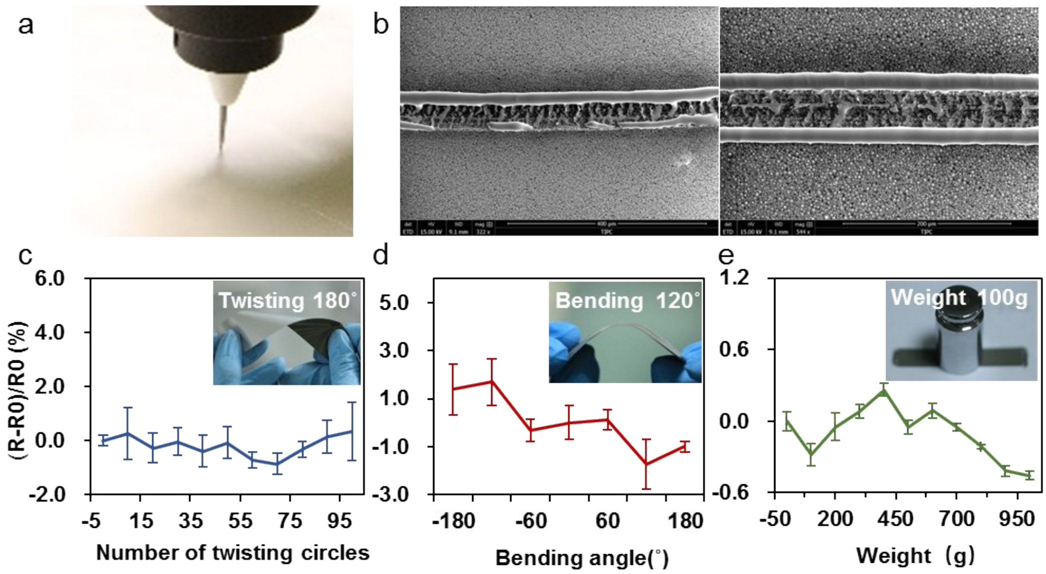

Figure S9. Needle engraved method. a) Setup used to write lines on the Janus film. b) SEM images of the written paths. c) Resistance change of needle engraved circuit when the sintered circuit is twisting multiple times. d) Resistance change of needle engraved circuit when the sintered circuit is bending. e) Resistance change of needle engraved circuit when applied different weight on the sintered circuit. The resistance changes of the needle engraved circuit under repeated twisting during 100 cycles are less than 2%, the resistance changes of the needle engraved circuit under bending are less than 3%, and the resistance changes of the needle engraved circuit when applying weight are maximally 0.5%.

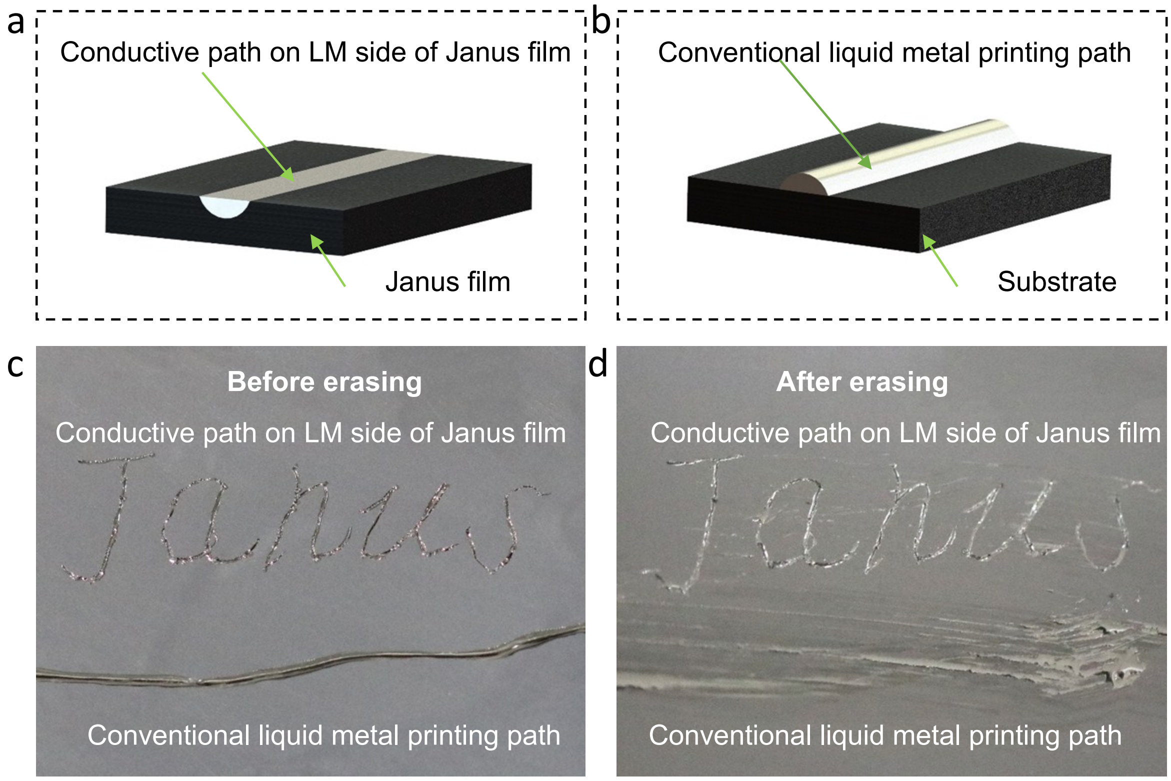

Figure S10. The stability of circuit fabricated in Janus film. a) The connected liquid metal conductive line is embedded in Janus film. b) Conventional liquid metal conductive line is usually printed on the surface of substrate. c) Conductive path fabricated with Janus film and conventional liquid metal printing path on the surface of Janus film. d) After erasing, conductive path still shows continuity and stability, while conventional liquid metal printing path was totally destroyed.

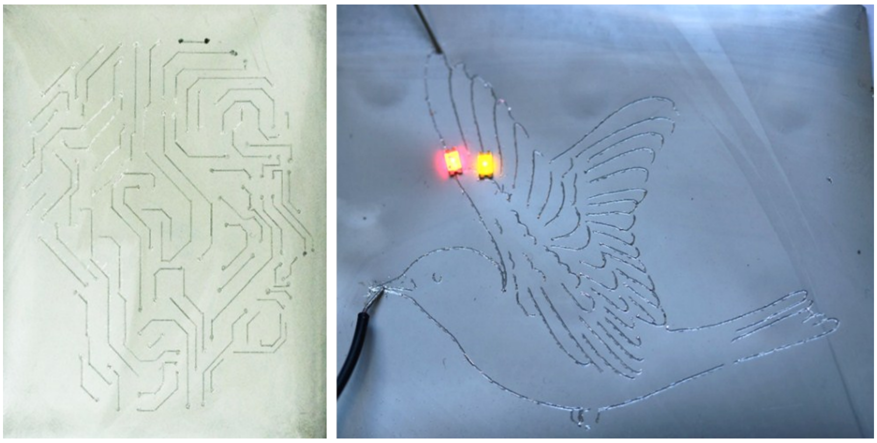

Figure S11. Other typical patterns fabricated on the thin and flexible LM Janus film using the wiping method.

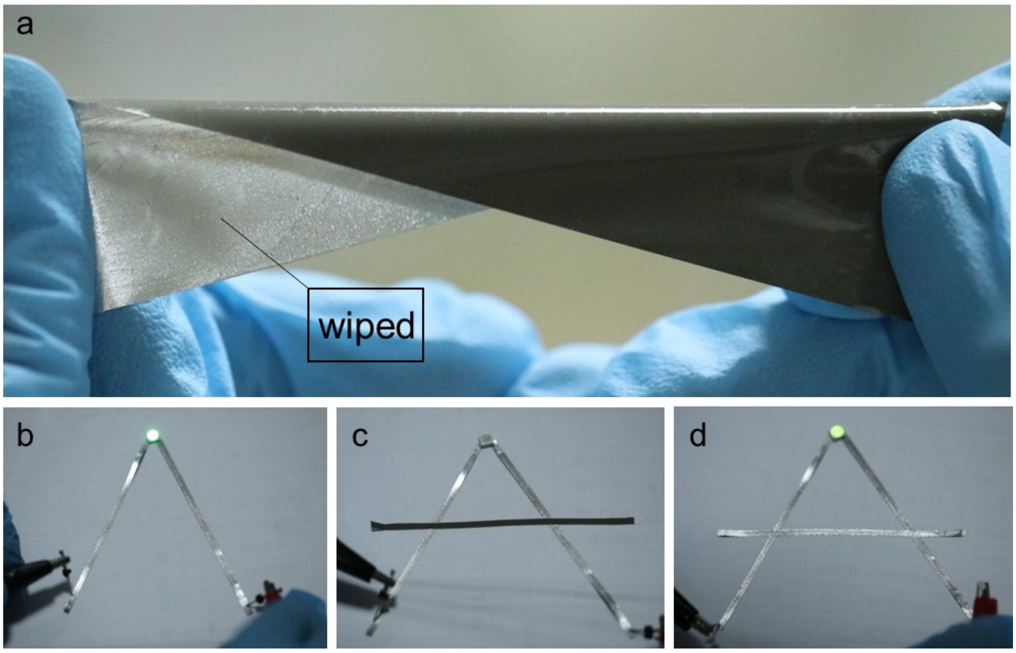

Figure S12. A simple example of wiped circuit with the LM Janus film. a) Janus strip with LM surface wiped. b) ~d) Janus strip with an insulating surface and a conductive surface gained from cutting wiped Janus film into strips. b) Triode lighted with strips as wire. c) Triode unlighted due to a short circuit caused by conductive surface of Janus strip. d) Triode lighted again by turning over the upper Janus strip.

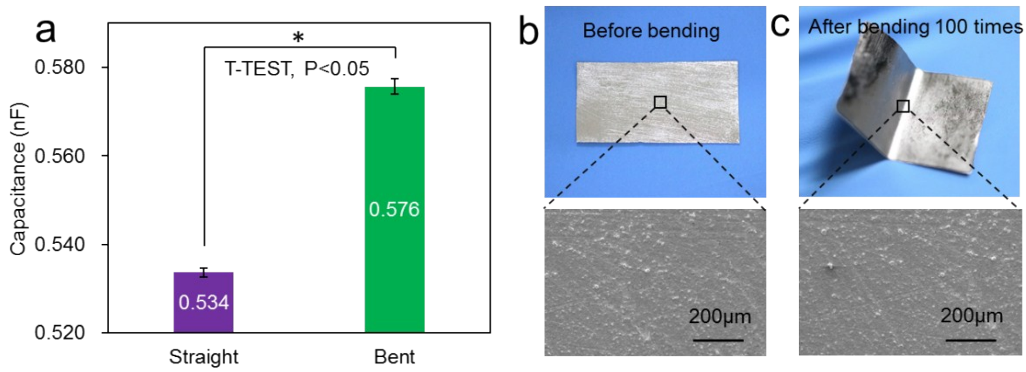

Figure S13. The durable and the structural change of the capacitor sensor made with wiped LM Janus films. a) Capacitance value when straightened and bent. The result of T-TEST shows a significant difference between the action of straightening and bending fingers. b) Morphology of the Janus film before bending test. c) Morphology of the Janus film after bending test.

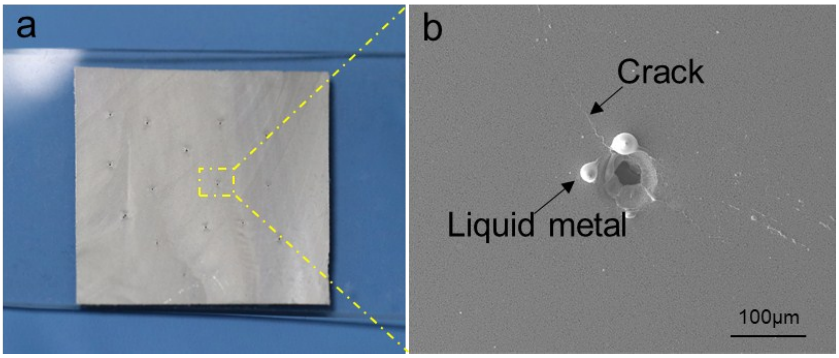

Figure S14. Morphology of the Janus film after punched. a) Macro view of the Janus film with many small holes. b) Microscopic SEM of the Janus film being punctured.

Movie description:

Movie S1. Flexible LM Janus film.

Movie S2. The natural deposition process of LM particles.

Movie S3. 3D X-ray Microscopes of the LM Janus film.

Movie S4. The analogue circuit achieving the lights function fabricated with the LM Janus film.

Movie S5. The ADTM fabricated with the LM Janus film.